DOI:10.1021/jf9028943

JOURNAL OF AGRICULTURAL AND FOOD CHEMISTRY
ARTICLE

Size Exclusion Chromatography To Gain Insight into the Complex Formation of Carrot Pectin Methylesterase and Its Inhibitor from Kiwi Fruit As Influenced by Thermal and High-Pressure Processing

Ruben P. Jolie, Thomas Duvetter, Philippe H. C. J. Verlinde, Sandy Van Buggenhout, Ann M. Van Loey, and Marc E. Hendrickx*

Laboratory of Food Technology and Leuven Food Science and Nutrition Research Centre (LFoRCe), Department of Microbial and Molecular Systems (M2S), Katholieke Universiteit Leuven, Kasteelpark Arenberg 22, P.B. 2457, B-3001 Leuven, Belgium

A size exclusion chromatography (HPSEC) method was implemented to study complex formation between carrot pectin methylesterase (PME) and its inhibitor (PMEI) from kiwi fruit in the context of traditional thermal and novel high-pressure processing. Evidence was gained that both thermal and high-pressure treatments of PME give rise to two distinct enzyme subpopulations: a catalytically active population, eluting from the size exclusion column, and an inactive population, aggregated and excluded from the column. When mixing a partly denatured PME sample with a fixed amount of PMEI, a PME−PMEI complex peak was observed on HPSEC, of which the peak area was highly correlated with the residual enzyme activity of the corresponding PME sample. This observation indicates complex formation to be restricted to the active PME fraction. When an equimolar mixture of PME and PMEI was subjected to either a thermal or a high-pressure treatment, marked differences were observed. At elevated temperature, enzyme and inhibitor remained united and aggregated as a whole, thus gradually disappearing from the elution profile. Conversely, elevated pressure caused the dissociation of the PME−PMEI complexes, followed by a separate action of pressure on enzyme and inhibitor. Remarkably, PMEI appeared to be pressure-resistant when compressed at acidic pH (ca. 4).

KEYWORDS: Pectin methylesterase (PME); pectin methylesterase inhibitor (PMEI); thermal and high-pressure denaturation; complex formation; HPSEC

INTRODUCTION

Pectin methylesterase (PME, EC 3.1.1.11) is an enzyme of either plant or microbial origin that catalyzes the demethoxylation of pectin, a major plant cell wall polysaccharide contributing to tissue integrity and rigidity. Through its action, PME alters the degree and pattern of methyl esterification of the linear homogalacturonan chains of pectin, releasing methanol (*1*). Plant PME is cell wall bound and, by pectin remodeling, plays diverse roles in both vegetative and reproductive plant development (*2*). From a food technological point of view, depending on the application, endogenous PME activity can have favorable as well as deleterious effects on the quality of plant-derived food products. For instance, demethoxylated pectin becomes a substrate for polygalacturonase (PG, EC 3.2.1.15), a pectinase that depolymerizes the pectin chain, inducing texture or viscosity loss (*3*). In the absence of PG, pectin with a low degree of methyl esterification can cross-link via divalent ion bridges to form intermolecular networks, promoting gel formation (*4*) but also causing cloud loss in fruit and vegetable juices (*5*−*7*). In addition, demethoxylation of pectin reduces its sensitivity to chemical β-eliminative depolymerization that can occur during heating (*4*, *8*, *9*). Hence, PME activity control is a major point of interest to meet specific quality targets for food products. Traditional thermal and novel high hydrostatic pressure processing have been shown to be valuable tools to direct PME-induced pectin conversions (through PME stimulation or inactivation) and, hence, to control pectin-related functional features of plant-derived food products in terms of structure, texture, rheology, and cloud stability (see, for example, refs *10*−*12*).

Both high-temperature and high-pressure can induce enzyme inactivation by perturbing the subtle balance of stabilizing intramolecular and solvent−protein interactions, leading to changes in the global enzyme conformation or at/near the active site (*13*). However, the denaturation mechanisms are substantially different. In thermoinactivation of enzymes, the universal first step is the (usually reversible) unfolding of the protein, being the result of counteracting hydrogen bonds, hydrophobic, ionic, and van der Waals interactions. Irreversibility is brought about by subsequent steps, which can entail noncovalent (aggregation or incorrect refolding) or covalent modifications and are highly specific for individual proteins (*14*). On the other hand,

*Corresponding author (telephone +32 16 321572; fax +32 16 321960; e-mail Marc.Hendrickx@biw.kuleuven.be).

 Published on Web 11/12/2009

high-pressure inactivation at ambient temperature is considered to be initiated by forcing water into the interior of the protein matrix, leading to conformational transitions and resulting in unfolding (*15*). Loss of native tertiary structure is predominantly ascribed to disruption of hydrophobic and electrostatic interactions. The large hydration changes accompanying these structural modifications are assumed to be the major source of volume decrease associated with pressure denaturation (*16*). Secondary structure changes occur only at very high pressure levels and cause irreversible denaturation (*13*), whereas covalent bonds of the primary structure are almost unaffected (*17*).

The discovery of a proteinaceous PME inhibitor (PMEI) in kiwi fruit (*Actinidia deliciosa*) (*18*) has added a new dimension to PME activity control. This PMEI was shown to be a glycoprotein of 152 (mainly acidic) amino acid residues, giving rise to a molar mass of 16.3 kDa and an acidic isoelectric pH (*19*, *20*). The inhibitor forms a reversible, noncovalent but highly polar 1:1 complex with all plant PMEs tested (*18*, *20*, *21*), but is ineffective against microbial PMEs (*22*−*24*). Elucidation of the three-dimensional structure of the complex between tomato PME and kiwi PMEI has established that PMEI covers the shallow cleft where the putative active site of the enzyme is located, thus preventing pectin binding (*25*). The physiological role of PMEI in vivo is not yet fully clarified. Due to the strong PME−PMEI interaction, kiwi PMEI can be exploited in affinity chromatography for laboratory-scale plant PME purification (*20*, *26*) and for inhibiting undesired PME activity in food applications, for example, to obtain cloud-stable juices (*27*). In addition, the discovery of this PMEI offers possibilities for the development of an innovative microscopic technique using labeled PMEI to localize endogenous PME in planta and to ameliorate the insight in the relationship between enzymatic pectin conversions and allied macroscopic properties (such as firmness and viscosity), both in model systems and in structured real food matrices. Nevertheless, for proper use of PMEI in PME inhibition or detection, thorough knowledge on the PME−PMEI interaction, as influenced by extrinsic process factors (such as high-temperature and high-pressure) is indispensable.

The objective of the current work was two-fold. On the one hand, the effect of a temperature- or pressure-induced denaturation of plant PME (i.e., carrot PME) on its subsequent complex formation with the proteinaceous inhibitor from kiwi fruit was investigated. On the other hand, the behavior of a PME−PMEI mixture upon thermal or high-pressure treatment was examined. Hereto, a high-performance size exclusion chromatography (HPSEC) method was implemented. As a prerequisite for reliable data interpretation, the behavior of denatured PME on HPSEC was investigated in advance, revealing some noteworthy information on the mechanism of PME inactivation.

MATERIALS AND METHODS

Materials. Young Belgian red carrots (*Daucus carota* cv. Sirena) and ripe kiwi fruits (*A. deliciosa* cv. Hayward) were purchased from a local supermarket. Carrot PME and kiwi PMEI were extracted and purified by affinity chromatography as described by Jolie et al. (*28*). For all further experiments, the main and most abundantly present carrot PME isozyme was isolated. Purified enzyme and inhibitor solutions were quickly frozen in liquid N_2 and stored at −80 °C until use.

Apple pectin (degree of esterification = 70−75%) was obtained from Fluka (Buchs, Switzerland). Ultrapure water (organic free, 18 MΩ cm resistance) was supplied by a Simplicity water purification system (Millipore, Billerica, MA). All other chemicals were of analytical grade.

Protein Determination. The protein content of the purified PME and PMEI solutions was determined according to Sigma procedure TPRO-562 using the bicinchoninic acid (BCA) kit (Sigma, Darmstadt, Germany). This method is based on the formation of a colored complex of BCA and Cu^+, after reduction of Cu^{2+} by proteins at alkaline pH. The complex was quantified spectrophotometrically at 562 nm and 25 °C (Ultrospec 2100 pro, GE Healthcare, Uppsala, Sweden). The protein concentration (mg/mL) was estimated by comparison with a standard curve of bovine serum albumin.

Thermal Treatments. Thermal treatments of protein solutions were performed in a temperature-controlled water bath. Protein samples were enclosed in 200 μL glass capillaries (Brand, Wertheim, Germany) to ensure isothermal heating. After a treatment of 5 min at different temperature levels, samples were withdrawn from the water bath and immediately cooled in ice water until further use.

High-Pressure Treatments. High-pressure treatments of protein solutions were conducted in a laboratory-scale high-pressure device (Resato, Roden, The Netherlands) consisting of eight cylindrical thermostated reactors (8 mL each). Propylene glycol (PG fluid, Resato) served as pressure-transmitting medium. Flexible microtubes (0.5 mL, Carl Roth, Karlsruhe, Germany) were filled with the protein solution and enclosed in the pressure reactors, already equilibrated to 25 °C. Pressure was built up slowly to 800 MPa (100 MPa/min, to minimize temperature increase due to adiabatic heating), and all pressure reactors were subsequently isolated. An equilibration period of 2 min was taken into account to allow temperature and pressure to evolve to the desired value. After preset time intervals (0−60 min), individual reactors were depressurized instantaneously, and samples were transferred to an ice water bath until analysis.

PME Activity Assay. PME activity was measured by an automatic pH-stat titration (Metrohm, Herisau, Switzerland) of the carboxyl groups formed during pectin hydrolysis, using 0.01 N NaOH. Routine assays were performed at pH 6.5 and 22 °C, using 30 mL of a 0.35% (w/v) apple pectin solution containing 0.117 M NaCl. By definition, one unit (U) of PME activity is the amount of enzyme catalyzing the de-esterification of 1 μmol of methyl ester bonds per minute under aforementioned conditions.

High-Performance Size Exclusion Chromatography. Size exclusion chromatography was performed on an Agilent 1200 series HPLC system (Agilent Technologies, Santa Clara, CA) with UV-DAD detection at 220 nm (G1315B, Agilent Technologies). Analytical HPLC was performed at 25 °C using a Superdex 75 10/300 GL column (300 × 10 mm, 13 μm average particle size, theoretical plates > 30000 m^{-1}, GE Healthcare). Elution was executed with 50 mM sodium phosphate buffer, pH 6.5, containing 150 mM NaCl at a flow rate of 0.45 mL/min for 55 min. Prior to injection (100 μL), protein samples were filtered through a syringe-driven filter unit (Millex-HV, PVDF, 0.45 μm, Millipore).

Experimental Setup. Two series of experiments were carried out. On the one hand, purified carrot PME (0.1 mg/mL in 50 mM sodium phosphate buffer, pH 6.5, containing 150 mM NaCl) was subjected to a thermal or high-pressure treatment. After treatment, bulk UV absorbance of the enzyme solutions was measured at 280 nm and 25 °C in quartz cells of 10 mm optical path length with a spectrophotometer (Ultrospec 2100 pro, GE Healthcare). Subsequently, each sample was divided into three parts. A first part was used for measuring the residual enzyme activity by pH-stat automatic titration, within 2 h after treatment. A second part was directly employed for HPSEC (as outlined in the previous section), whereas a third part was mixed with a minor molar excess of (untreated) kiwi PMEI, prior to filtration and injection on the size exclusion column.

On the other hand, an equimolar mixture of purified carrot PME (0.1 mg/mL) and kiwi PMEI was thermally or high-pressure treated. For thermal experiments, PME−PMEI mixtures were diluted in sodium phosphate buffer, pH 6.5. High-pressure experiments were carried out both in sodium phosphate, pH 6.5, and MES−NaOH, pH 6.5. All buffers had a 50 mM concentration and contained 150 mM NaCl. MES [2-(*N*-morpholino)ethanesulfonic acid] buffer was selected because of its putative pressure stability, that is, the ability to maintain the set pH upon pressurization (*29*), in contrast to sodium phosphate buffer. After treatment, bulk UV absorbance at 280 nm and 25 °C was measured for each sample. Subsequently, all treated PME−PMEI samples were analyzed by HPSEC.

For selected conditions, experiments were done in duplicate. All parameters measured showed good reproducibility.

Data Analysis. Although enzyme inactivation and protein denaturation due to thermal or high-pressure processing are complex processes

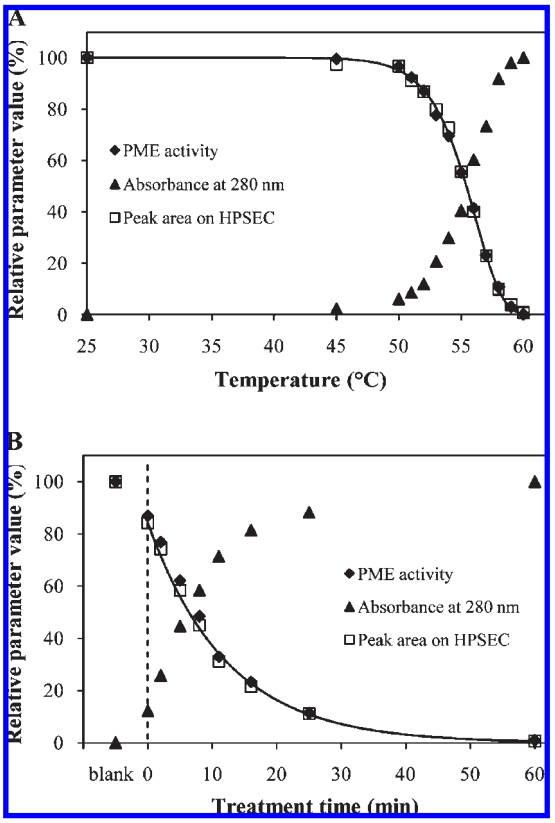

Figure 1. Effect of a thermal treatment (5 min at different temperatures) (**A**) and a high-pressure treatment (different time intervals at 800 MPa and 25 °C) (**B**) of purified carrot PME on the residual PME activity, UV absorbance at 280 nm, and residual peak area on HPSEC. Values relative to the maximal parameter value are depicted. Full lines represent the best fit of the residual PME peak area to the first-order model. Time 0 min (dashed line) refers to the start of isothermal−isobaric conditions of the high-pressure treatment.

involving several events, kinetics often obey a simple first-order model (*16*):

$$A = A_0 \exp(-kt)$$

with A the measured response (e.g., enzyme activity) and k the reaction rate constant (min^{-1}). The temperature sensitivity of the rate constant can be described by the Arrhenius equation and is expressed in terms of activation energy (E_a):

$$k = k_{ref} \exp\left[\frac{E_a}{R}\left(\frac{1}{T_{ref}} - \frac{1}{T}\right)\right]$$

where k_{ref} is the rate constant at reference temperature T_{ref} (K), E_a the activation energy (J/mol), and R the universal gas constant.

Nonlinear regression analysis was applied to estimate the kinetic parameters on the basis of the experimental data (SAS Statistical Software version 9.1). For the thermal treatments (constant treatment time at different treatment temperatures), a one-step regression approach was employed, in which the Arrhenius equation was introduced in the first-order model to describe the course of the response A as a function of treatment temperature.

RESULTS AND DISCUSSION

Thermal and High-Pressure Denaturation of Carrot PME. The behavior of denatured PME on HPSEC was investigated. Hereto, a set of PME samples with different degrees of irreversible denaturation was prepared by subjecting purified carrot PME solutions to a thermal or high-pressure treatment. Subsequently to the treatment, UV absorbance of the PME solution (at 280 nm) as well as residual enzyme activity and residual peak area at 220 nm on HPSEC were determined.

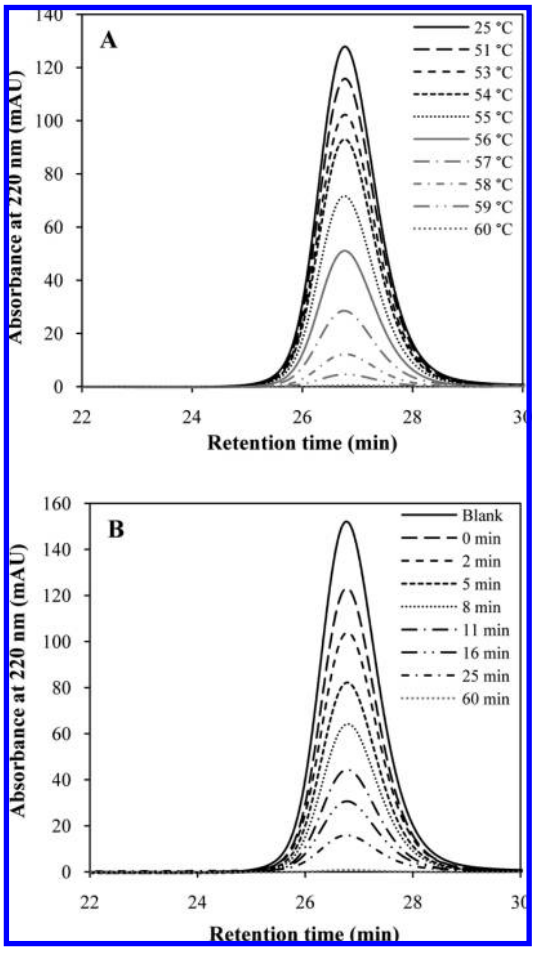

Figure 2. Size exclusion chromatograms of purified carrot PME after (**A**) thermal treatment (5 min at different temperature levels) and (**B**) high-pressure treatment (different time intervals at 800 MPa and 25 °C). "Blank" refers to the untreated sample and "0 min" to the start of the isothermal−isobaric conditions of the high-pressure treatment.

First, PME samples were treated for 5 min at different temperature levels (25−60 °C) and atmospheric pressure. Increasing the intensity of the thermal treatment caused a gradual loss of enzyme activity (**Figure 1A**), strictly obeying first-order kinetics, in agreement with data from the kinetic inactivation study of carrot PME reported previously (*28*). A series of 13 PME samples with a residual activity in the range from 100 to 0%, relative to the untreated PME sample (25 °C), was obtained. Along with the decrease in enzyme activity, the relative absorbance of the protein solutions at 280 nm increased (**Figure 1A**). When residual enzyme activity was plotted versus relative absorbance, a straight line with a slope of −1.001 and R^2 of 0.997 was obtained (not shown), revealing a markedly high correlation between both parameters. In addition, size exclusion chromatography was performed for all thermally treated PME samples. **Figure 2A** presents an overlay of a selected number of chromatograms. In all cases (blank and treated samples), a single peak (retention time = 26.77 ± 0.01 min) was observed in the entire elution period. The area of this PME peak was calculated and plotted relative to the untreated PME (**Figure 1A**). The residual peak area decreased with rising treatment temperature, obeying first-order kinetics. By means of nonlinear one-step regression analysis (Corr R^2 = 0.999), the rate constant at a T_{ref} of 55 °C ($k_{55°C}$ = 0.114 ± 0.002 min^{-1}) and the activation energy

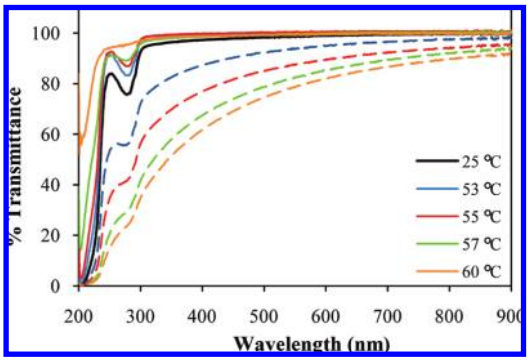

Figure 3. Effect of a thermal treatment of purified carrot PME (5 min at different temperature levels) on the optical transmittance spectrum of the enzyme solution, recorded before and after centrifugation (dashed and solid lines, respectively).

(E_a = 424.4 ± 9.8 kJ/mol) were estimated. A particularly high correlation (slope = 1.003; R^2 = 0.999) between residual enzyme activity and residual peak area was obtained.

Analogously, for high-pressure inactivation, a set of nine carrot PME samples with residual enzymatic activities between 100 and 1%, relative to the untreated PME sample, was obtained by treating the enzyme solutions for different time intervals (0−60 min) at 800 MPa and 25 °C (**Figure 1B**). In accordance with former data, a first-order decay was followed (*28*). Compared to the temperature-treated samples, similar observations could be made. A single peak of PME (retention time = 26.78 ± 0.02 min) was detected on the size exclusion chromatograms (**Figure 2B**). Residual enzyme activity was inversely correlated with relative bulk absorbance at 280 nm (slope = −1.011; R^2 = 0.993), whereas it was directly correlated with the PME peak area on HPSEC (slope = 1.012; R^2 = 0.998) (**Figure 1B**). The first-order rate constant for the reduction in PME peak area was estimated at k_{800MPa} = 0.082 ± 0.002 min^{-1} (Corr R^2 = 0.999).

To elucidate the perceived increase in bulk UV absorbance of the PME solutions after treatment, optical transmittance spectra (%*T* in the 200−900 nm range) of selected samples were recorded, before and after centrifugation (10 min at 15000*g*). Spectra for a number of thermally treated enzyme samples are presented in **Figure 3**. Similar results were obtained for pressure-treated PME (results not shown). In contrast to the overall decrease in %*T* for the noncentrifuged samples (i.e., throughout the spectrum), an increase in %*T* was observed after centrifugation, mainly in the 200−280 nm region of the spectrum (i.e., the part of the spectrum where peptide bonds and aromatic amino acids absorb light). This observation can be explained by the processing-induced formation of protein aggregates, which cause light scattering and an increase in apparent UV absorbance to take place (*30*) but can be removed by centrifugation, without loss of enzyme activity or decrease of the PME peak area on HPSEC. This aggregation tendency is usually attributed to the intermolecular interaction of hydrophobic sites (previously buried in the protein interior) as an answer to their thermodynamically unfavorable exposure to the aqueous surrounding medium upon conversion of the native to the denatured protein form (*14*). Temperature-induced aggregation following unfolding was also demonstrated for recombinant *Aspergillus aculeatus* PME by means of Fourier transform infrared (FTIR) spectroscopy, however, at a markedly higher protein concentration (20 mg/mL in D_2O) (*31*, *32*).

Because the presence of NaCl may promote chemical and physical protein aggregation due to a decreased intermolecular repulsion (*33*), aggregation behavior accompanying irreversible inactivation of PME was followed spectrophotometrically in the presence and absence of 150 mM NaCl. No significant differences in optical transmittance and residual enzyme activity were observed, ruling out a major influence of NaCl on the inactivation process of the purified carrot PME studied here.

The above results bear the evidence for the occurrence of processing-induced formation of PME aggregates. Nevertheless, no high molecular mass components were detected by size exclusion chromatography on the Superdex 75 column, either in protein samples that underwent filtration or centrifugation prior to injection or in samples without a preceding clearance step. In an additional experiment it was shown that sample filtration and sample centrifugation resulted in the same residual PME peak areas (R^2 > 0.997 for both thermal and high-pressure inactivation) and that sample clearance was not accompanied by loss of enzyme activity. The fact that the aggregates can be removed by filtration through a 0.45 μm filter and that they are excluded from the size exclusion column in the case of omission of the preparatory clearance step suggests a high molecular mass of the protein assemblies (> dimer or trimer).

All foregoing results reveal that a partly irreversibly denatured PME sample, either thermally or high-pressure treated, basically exists of two distinct subpopulations. One PME subpopulation is eluting from the size exclusion column and has a peak area that is highly correlated to the enzymatic activity of the sample, indicating that this subpopulation is associated with the active PME fraction. A second subpopulation, however, does not appear in the chromatogram. This subpopulation does not account for any residual PME activity and, hence, can be considered the inactive, irreversibly denatured enzyme fraction. As described above, this inactive PME fraction consists of enzyme aggregates and is mainly removed during the routine filtration step prior to sample application on the HPLC column.

Remarkably, the present study shows little difference in the results for thermal and high-pressure inactivation, despite the substantial differences in the denaturation mechanisms (cf. Introduction). Although it is observed that aggregation results less frequently from pressure than from heat treatment, which may be explained by the fact that in the latter case unfolding is the first step in the denaturation process, prior to water penetration (*15*), irreversible high-pressure inactivation of PME appears also to be accompanied by aggregate formation, even at the relatively low protein concentration used here (i.e., 0.1 mg/mL). However, since pressure-induced protein gels have characteristics different from the temperature-induced ones (*34*), it seems plausible that the pressure-induced aggregate is different from that induced thermally at 0.1 MPa. Whether or not differing, none of either type of aggregation appears to invade the independent behavior of the active PME population with regard to enzyme activity and size exclusion separation.

Inactivation kinetic studies are traditionally restricted to the population level (see, for example, ref *10*). Only the ensemble average activity is described as a function of the relevant process parameters. The same holds true for monitoring modifications of the protein conformation by FTIR spectroscopy. Insight into the distribution of the intensity of structural damage and, hence, the distribution of activity in the population is lacking. In this context, the current results give indirect proof that, postfactum, a partly irreversibly denatured bulk PME sample is basically inhomogeneous, consisting of enzymes in either a fully active or a fully inactive state. So, when inactivating a bulk enzyme solution, certain individual enzyme molecules will unfold (and presumably aggregate), whereas others will preserve their native, catalytically active state. To extract information on the pathway followed by an individual enzyme molecule to finally reach the irreversibly

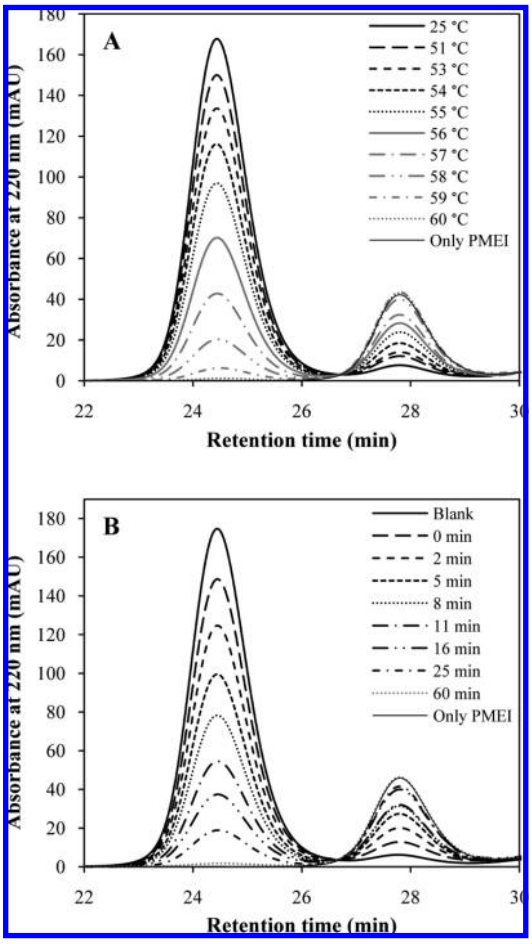

Figure 4. Size exclusion chromatograms of the mixture of a fixed amount of untreated kiwi PMEI with purified carrot PME that underwent (**A**) a thermal treatment (5 min at different temperature levels) and (**B**) a high-pressure treatment (different time intervals at 800 MPa and 25 °C). "Only PMEI" refers to the chromatogram of a PMEI sample without PME, "blank" to the untreated sample, and "0 min" to the start of the isothermal−isobaric conditions of the high-pressure treatment.

inactivated state, recent techniques such as single-molecule fluorescence spectroscopy may be appropriate (*35*).

Effect of PME Denaturation on PME−PMEI Complex Formation. The complex formation between carrot PME and kiwi PMEI, and more precisely the way the interaction is influenced by a preceding temperature- or pressure-induced irreversible denaturation of PME, was investigated by means of HPSEC. A broad set of partially denatured PME samples with residual enzyme activities ranging from 100 to 0% was prepared by thermal or high-pressure treatment, as described above. Subsequently, these samples were incubated with a fixed amount of purified kiwi PMEI, corresponding to a minor molar excess of the inhibitor, prior to sample filtration and application on the size exclusion column. A previous study assured good complex formation at the pH (i.e., 6.5) and NaCl concentration (i.e., 150 mM) of the elution buffer used for the HPSEC analysis (*28*).

Chromatograms were recorded for both thermally (**Figure 4A**) and high-pressure (**Figure 4B**) treated enzyme solutions. In all cases, two separate peaks with retention times 24.45 ± 0.02 and 27.82 ± 0.02 min were obtained, originating from the PME−PMEI complex and free PMEI, respectively. As expected, on the basis of the respective molar masses, the retention time of free PME (26.77 min, cf. previous section) was intermediate to the ones of PME−PMEI complex and free PMEI. Increasing the

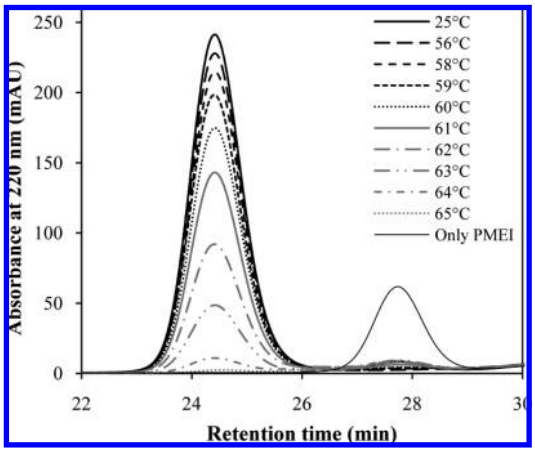

Figure 5. Size exclusion chromatograms of an equimolar mixture of carrot PME and kiwi PMEI after thermal treatment (5 min at different temperature levels). "Only PMEI" refers to the chromatogram of untreated PMEI without PME.

treatment intensity (i.e., treatment temperature or pressurization time) caused the complex peak to reduce, whereas the PMEI peak enlarged. Remarkably, the decline in complex peak area was highly correlated with the decrease in residual enzyme activity (slope = 1.011 and R^2 = 0.999 for thermally treated PME; slope = 1.018 and R^2 = 0.996 for pressure-treated PME), as was the increase in PMEI peak area. The chromatogram of a mixture of PMEI and fully inactivated PME coincided with the one of a mixture of PMEI and buffer.

The amount of complex that can be formed between PME and PMEI after a (partial) denaturation of PME proves to be strongly associated with the residual activity of the enzyme sample. Moreover, all PMEI that is mixed with the PME sample and applied on the column is afterward retrieved in the effluent. Although, during sample preparation, PMEI comes into contact with the entire PME population after processing, assumed to consist of individual active and aggregated inactive PME molecules (cf. previous section), all PMEI molecules elute from the column in the company of the active PME fraction. Thereby, a part of the PMEI is bound to PME, another part is not (the ratio depending on the amount of PME available for complex formation, determined by the degree of enzyme inactivation). None of the inhibitor is associated with the aggregated inactive enzyme fraction and, hence, removed by filtration prior to injection.

The whole of these observations unequivocally demonstrates that complex formation is limited to the active PME fraction, whereas the inactivated (and aggregated) PME fraction does not bind to PMEI anymore. Hence, in the context of PME inactivation, the PME−PMEI binding can be considered an "activity-associated" binding. This statement of a strong link between enzyme activity and susceptibility toward complexation/inhibition is endorsed by the observation that PMEI covers the putative active site cleft upon complex formation (*25*). Upon PME inactivation, the active site of the enzyme is torn apart or becomes inaccessible for both substrate and inhibitor molecules. Consequently, the intrinsically strong enzyme−inhibitor linkage is rendered completely impossible.

Effect of Thermal Treatment on the PME−PMEI Complex. To examine the behavior of the PME−PMEI complex upon thermal processing, an equimolar mixture of carrot PME and kiwi PMEI (in sodium phosphate buffer, pH 6.5) was treated for 5 min at temperature levels between 25 and 65 °C. Afterward, UV absorbance of the protein solution (at 280 nm) was measured and size exclusion chromatograms (**Figure 5**) were recorded. A major peak

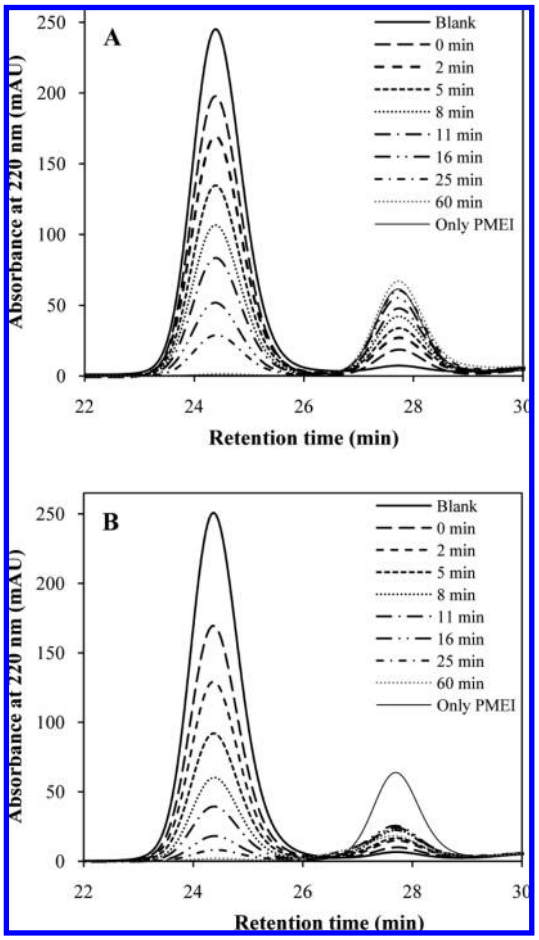

Figure 6. Size exclusion chromatograms of an equimolar mixture of carrot PME and kiwi PMEI after high-pressure treatment (800 MPa and 25 °C for different treatment times) in (**A**) sodium phosphate buffer, pH 6.5, and (**B**) MES−NaOH buffer, pH 6.5. "Only PMEI" refers to the chromatogram of untreated PMEI without PME.

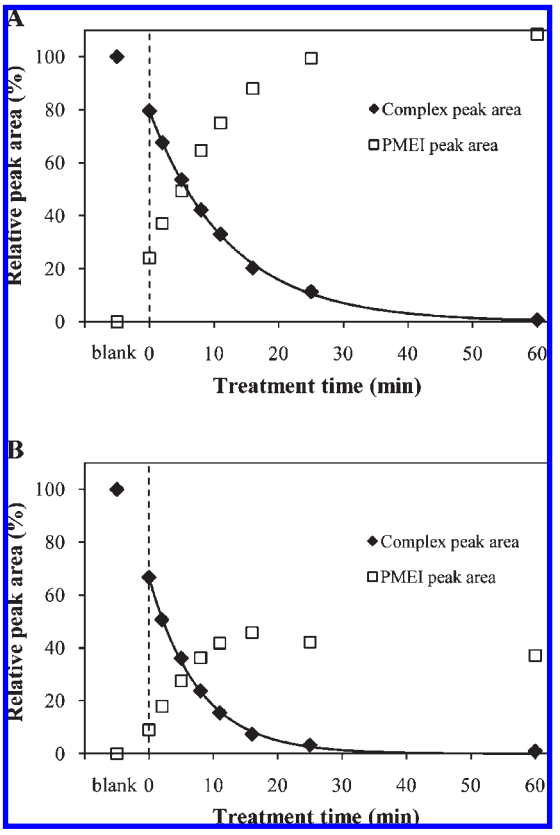

Figure 7. Effect of a high-pressure treatment (different time intervals at 800 MPa and 25 °C) of an equimolar mixture of carrot PME and kiwi PMEI in sodium phosphate buffer, pH 6.5 (**A**), and MES buffer, pH 6.5 (**B**), on the HPSEC peak areas of the PME−PMEI complex and free PMEI. Peak areas relative to those of untreated complex and untreated PMEI, respectively, are depicted. Full lines represent the best fit of the residual complex peak area to the first-order model. Time 0 min (dashed line) refers to the start of isothermal−isobaric conditions.

at retention time 24.42 ± 0.02 min and a minor peak around 27.78 ± 0.04 min could be distinguished, corresponding to PME−PMEI complex and free PMEI, respectively. Increasing the treatment temperature caused a reduction in the complex peak area, whereas the PMEI peak remained negligible compared to the peak of PMEI without PME ("only PMEI"). Simultaneously, UV absorbance of the protein solutions at 280 nm increased with rising temperature (inversely correlated with the complex peak area with slope = −1.084 and R^2 = 0.996), indicating aggregation to take place. Notably, the decline in complex peak area could adequately be described by a first-order model. Nonlinear one-step regression analysis (Corr R^2 = 0.999) allowed estimation of the rate constant at a T_{ref} of 61 °C ($k_{61°C}$ = 0.112 ± 0.002 min^{-1}) and the activation energy (E_a = 487.7 ± 12.9 kJ/mol).

From the above results it can be concluded that, upon heat treatment of the PME−PMEI complex, enzyme and inhibitor are not driven apart. Yet, the complex is denatured (and aggregated) as one entity, following first-order kinetics. Furthermore, in comparison with the thermal denaturation of carrot PME in the absence of kiwi PMEI (cf. supra), denaturation of the PME−PMEI complex is only initiated at higher temperature levels (a difference of 6 °C to obtain the same k value). The temperature sensitivity, however, is similar, judging by E_a values in the same order of magnitude. The presence of PMEI seems to have a slight protective effect on PME with regard to thermal denaturation. The lack of evidence for thermal dissociation of the PME−PMEI complex confirms an earlier indication in that direction based on activity measurements of PME in the presence of PMEI at elevated temperatures (*28*).

Effect of High-Pressure Treatment on the PME−PMEI Complex. To address the scientific question of how the PME−PMEI complex behaves at elevated pressure, an equimolar mixture of carrot PME and kiwi PMEI was subjected to a pressure level of 800 MPa for different times (0−60 min) at 25 °C. Subsequently, UV bulk absorbance (280 nm) was measured and samples were analyzed by HPSEC. Experiments were performed both in sodium phosphate buffer, pH 6.5, and in MES buffer, pH 6.5. MES buffer will maintain its preset pH value of 6.5 even at elevated pressure levels ("pressure-stable"), whereas pressurization will cause a pH drop in the ("pressure-labile") phosphate buffer (∼−0.3 units per 100 MPa) due to pressure-induced ionization of weak acids (*36*).

Figure 6A represents the chromatograms of the PME−PMEI complex after high-pressure treatment in the pressure-labile sodium phosphate buffer. Peaks of PME−PMEI complex (24.39 ± 0.01 min) and peaks of free PMEI (27.73 ± 0.01 min) were observed. The evolution of peak areas with treatment time, relative to those of untreated samples, is depicted in **Figure 7A**. With prolonged treatment time, the residual complex peak area showed a first-order decrease (k = 0.081 ± 0.001 min^{-1}, Corr R^2 = 0.999). Meanwhile, the free PMEI peak area steadily augmented until an area even slightly larger than the one of untreated

PMEI ("only PMEI") was reached. A concomitant increase in bulk UV absorbance (data not shown) pointed to the occurrence of a pressure-induced formation of protein aggregates.

High-pressure processing of the PME−PMEI mixture in a pressure-labile buffer causes the amount of enzyme−inhibitor complex to diminish with treatment time. Remarkably, the rate of this decline is in strong accordance with the rate at which the PME peak decreases when PME undergoes a similar high-pressure treatment (cf. supra). This agreement indicates that the residual amount of PME−PMEI complex most likely is governed by the inactivation of the PME, because only active PME molecules can bind to the inhibitor (as stated above). Moreover, coincidence of the chromatogram of the maximally treated PME−PMEI mixture with the one of untreated PMEI demonstrates that all PMEI initially present in the protein mixture also elutes from the column. The following hypothesis can be put forward to explain the whole of the observations. During pressurization, the enzyme−inhibitor complexes present in the PME−PMEI mixture dissociate. PME undergoes first-order inactivation in line with its behavior in the absence of PMEI. Conversely, PMEI is not obliterated by a pressure level of 800 MPa when dissolved in a pressure-labile phosphate buffer. This finding was successfully confirmed by HPSEC analysis of pressure-treated PMEI samples (data not shown) and was in conformity with a previous study based on measurements of residual PMEI inhibitory capacity (*28*). After decompression, PME−PMEI complexes are formed again to a maximal extent, depending on the residual amount of active PME. In all cases, an excess of PMEI is generated in the pressure-treated samples.

To assess whether observations are governed by pressure-induced pH changes in the protein solution, chromatograms of the PME−PMEI complex after high-pressure treatment in the pressure-stable MES buffer were recorded likewise (**Figure 6B**). Peaks of PME−PMEI complex (24.39 ± 0.02 min) and peaks of free PMEI (27.70 ± 0.02 min) were detected, and the course of their integrated areas was plotted versus treatment time (**Figure 7B**). The longer the treatment lasted, the lower the residual complex peak area was (first-order decay with $k = 0.130 \pm 0.002\ \text{min}^{-1}$, Corr $R^2 = 0.999$). Besides, the PMEI peak area gradually expanded until a plateau level was attained (~ 40% of the untreated "only PMEI" peak). These changes in the proportions of peak areas were accompanied by an increase in apparent bulk UV absorbance of the samples (data not shown), indicative of light scattering by protein aggregates.

As for the pressure-labile buffer system, the amount of PME−PMEI complex retrieved after processing in the pressure-stable MES buffer decreases and a pressure-induced dissociation of the enzyme−inhibitor complexes can be assumed. Upon decompression, residual active PME engages with residual PMEI to form as many complexes as possible. Since the amount of complex follows first-order kinetics as a function of treatment time, as does the residual PME peak area under similar conditions (cf. supra), the amount of native PME most likely is the limiting factor. However, the rate at which the complex peak area is reduced is higher than the degradation rate of pure PME, subjected to a comparable pressure treatment. So, in one way or another, the presence of PMEI seems to promote the denaturation of PME. Furthermore, in all samples, an excess amount of PMEI is detected. However, not all of the initially present PMEI can be retrieved in the chromatogram. This indicates that, in contrast to the results in the pressure-labile buffer, PMEI is not fully stable in the MES buffer. A plateau level of approximately 40% of the initial amount is reached after extended treatment times, suggesting the existence of a processing-stable PMEI fraction. This finding is in accordance with an earlier study on the high-pressure stability of kiwi PMEI, based on inhibitory capacity measurements (*28*).

The results described in this section make it clear that pH (in the range from approximately 4 to 6.5) significantly influences the high-pressure behavior of a PME−PMEI mixture. Nevertheless, irrespective of the buffer system used, there is marked evidence for a dissociation of the PME−PMEI complex due to high-pressure application, and high-pressure treatment of an equimolar mixture of PME and PMEI (at the conditions studied here) will anyhow give cause for an excess amount of PMEI.

Conclusion. Size exclusion chromatography of (partially) denatured carrot PME indicated that two distinct subpopulations of PME molecules are present in thermally or high-pressure treated enzyme solutions. Only the active PME subpopulation is capable of binding to the kiwi PME inhibitor. This observation suggests that a PMEI probe would bind to endogenous PME in plant tissue, both before and after processing, as long as the enzyme possesses activity, hence enabling detection of all endogenous PME activity. Furthermore, postprocessing addition of kiwi PMEI to a food product would allow binding and presumably inhibiting residual undesired PME, for example, to obtain cloud-stable fruit and vegetable juices.

HPSEC was also successfully applied to study the behavior of the PME−PMEI complex at elevated temperature or pressure levels. Heat treatment proves not to dissociate the complex, but rather to denature the complex as one entity. By contrast, high-pressure treatment induces disunion of enzyme and inhibitor, followed by gradual inactivation of PME and PMEI, the latter showing pH-dependent inactivation characteristics. The findings especially open perspectives for preprocessing addition of kiwi PMEI to food systems in combination with high-pressure processing, particularly in (high) acid foods. However, further experiments are required to confirm whether these in vitro conclusions are transferable to real food matrices.

ACKNOWLEDGMENT

Prof. Karel Heremans and Prof. Filip Meersman are gratefully acknowledged for the fruitful discussions on protein denaturation and enzyme inactivation.

LITERATURE CITED

(1) Ridley, B. L.; O'Neill, M. A.; Mohnen, D. A. Pectins: structure, biosynthesis, and oligogalacturonide-related signaling. *Phytochemistry* **2001**, *57* (6), 929–967.

(2) Pelloux, J.; Rusterucci, C.; Mellerowicz, E. J. New insights into pectin methylesterase structure and function. *Trends Plant Sci*. **2007**, *12* (6), 267–277.

(3) Rexova-Benkova, L.; Markovic, O. Pectic enzymes. *Adv. Carbohydr. Chem. Biochem*. **1976**, *33*, 323–385.

(4) Van Buren, J. P. The chemistry of texture in fruits and vegetables. *J. Texture Stud*. **1979**, *10*, 1–23.

(5) Krop, J. P. P.; Pilnik, W. Effect of pectic acid and bivalent cations on cloud loss of citrus juice. *Lebensm. -Wiss. Technol*. **1972**, *7*, 62–63.

(6) Versteeg, C.; Rombouts, F. M.; Spaansen, C. H.; Pilnik, W. Thermostability and orange juice cloud destabilizing properties of multiple pectinesterases from orange. *J. Food Sci*. **1980**, *45* (4), 969–998.

(7) Sims, C. A.; Balaban, M. O.; Matthews, R. F. Optimization of carrot juice color and cloud stability. *J. Food Sci*. **1993**, *58* (5), 1129–1131.

(8) Keijbets, M. J.; Pilnik, W. β-Elimination of pectin in presence of anions and cations. *Carbohydr. Res*. **1974**, *33* (2), 359–362.

(9) Sajjaanantakul, T.; Van Buren, J. P.; Downing, D. L. Effect of methyl-ester content on heat degradation of chelator-soluble carrot pectin. *J. Food Sci*. **1989**, *54* (5), 1272–1277.

(10) Duvetter, T.; Sila, D. N.; Van Buggenhout, S.; Jolie, R.; Van Loey, A.; Hendrickx, M. Pectins in processed fruit and vegetables.

Part I − Stability and catalytic activity of pectinases. *Compr. Rev. Food Sci. Food Saf.* **2009**, *8* (2), 75–85.
(11) Sila, D. N.; Van Buggenhout, S.; Duvetter, T.; Fraeye, I.; De Roeck, A.; Van Loey, A.; Hendrickx, M. Pectins in processed fruit and vegetables. Part II − Structure−function relationships. *Compr. Rev. Food Sci. Food Saf.* **2009**, *8* (2), 86–104.
(12) Van Buggenhout, S.; Sila, D. N.; Duvetter, T.; Van Loey, A.; Hendrickx, M. Pectins in processed fruits and vegetables. Part III − Texture engineering. *Compr. Rev. Food Sci. Food Saf.* **2009**, *8* (2), 105–117.
(13) Balny, C.; Masson, P. Effects of high-pressure on proteins. *Food Rev. Int.* **1993**, *9* (4), 611–628.
(14) Klibanov, A. M. Stabilization of enzymes against thermal inactivation. *Adv. Appl. Microbiol.* **1983**, *29*, 1–28.
(15) Balny, C.; Masson, P.; Heremans, K. High pressure effects on biological macromolecules: from structural changes to alteration of cellular processes. *BBA−Protein Struct. Mol. Enzymol.* **2002**, *1595* (1−2), 3–10.
(16) Ludikhuyze, L.; Van Loey, A.; Indrawati; Smout, C.; Hendrickx, M. Effects of combined pressure and temperature on enzymes related to quality of fruits and vegetables: from kinetic information to process engineering aspects. *Crit. Rev. Food Sci. Nut.* **2003**, *43* (5), 527–586.
(17) Heremans, K. The behaviour of proteins under pressure. In *High Pressure Chemistry, Biochemistry and Materials Science*; Winter, R., Jonas, J., Eds.; Kluwer Academic Publishers: Dordrecht, The Netherlands, 1993; pp 443−469.
(18) Balestrieri, C.; Castaldo, D.; Giovane, A.; Quagliuolo, L.; Servillo, L. A glycoprotein inhibitor of pectin methylesterase in kiwi fruit (*Actinidia chinensis*). *Eur. J. Biochem.* **1990**, *193* (1), 183–187.
(19) Camardella, L.; Carratore, V.; Ciardiello, M. A.; Servillo, L.; Balestrieri, C.; Giovane, A. Kiwi protein inhibitor of pectin methylesterase − amino-acid sequence and structural importance of two disulfide bridges. *Eur. J. Biochem.* **2000**, *267* (14), 4561–4565.
(20) Giovane, A.; Balestrieri, C.; Quagliuolo, L.; Castaldo, D.; Servillo, L. A glycoprotein inhibitor of pectin methylesterase in kiwi fruit − purification by affinity chromatography and evidence of a ripening-related precursor. *Eur. J. Biochem.* **1995**, *233* (3), 926–929.
(21) Ly-Nguyen, B.; Van Loey, A. M.; Smout, C.; Verlent, I.; Duvetter, T.; Hendrickx, M. E. Effect of intrinsic and extrinsic factors on the interaction of plant pectin methylesterase and its proteinaceous inhibitor from kiwi fruit. *J. Agric. Food Chem.* **2004**, *52*, 8144–8150.
(22) Duvetter, T.; Van Loey, A.; Smout, C.; Verlent, I.; Ly-Nguyen, B.; Hendrickx, M. *Aspergillus aculeatus* pectin methylesterase: study of the inactivation by temperature and pressure and the inhibition by pectin methylesterase inhibitor. *Enzyme Microb. Technol.* **2005**, *36* (4), 385–390.
(23) Giovane, A.; Servillo, L.; Balestrieri, C.; Raiola, A.; D'Avino, R.; Tamburrini, M.; Ciardiello, M. A.; Camardella, L. Pectin methylesterase inhibitor. *BBA−Proteins Proteom.* **2004**, *1696* (2), 245–252.
(24) D'Avino, R.; Camardella, L.; Christensen, T. M. I. E.; Giovane, A.; Servillo, L. Tomato pectin methylesterase: modeling, fluorescence, and inhibitor interaction studies − comparison with the bacterial (*Erwinia chrysanthemi*) enzyme. *Proteins* **2003**, *53* (4), 830–839.
(25) Di Matteo, A.; Giovane, A.; Raiola, A.; Camardella, L.; Bonivento, D.; De Lorenzo, G.; Cervone, F.; Bellincampi, D.; Tsernoglou, D. Structural basis for the interaction between pectin methylesterase and a specific inhibitor protein. *Plant Cell* **2005**, *17* (3), 849–858.
(26) Ly-Nguyen, B.; Van Loey, A. M.; Smout, C.; Ozcan, S. E.; Fachin, D.; Verlent, I.; Truong, S. V.; Duvetter, T.; Hendrickx, M. E. Mild-heat and high-pressure inactivation of carrot pectin methylesterase: a kinetic study. *J. Food Sci.* **2003**, *68* (4), 1377–1383.
(27) Castaldo, D.; Lovoi, A.; Quagliuolo, L.; Servillo, L.; Balestrieri, C.; Giovane, A. Orange juices and concentrates stabilization by a proteic inhibitor of pectin methylesterase. *J. Food Sci.* **1991**, *56* (6), 1632–1634.
(28) Jolie, R. P.; Duvetter, T.; Houben, K.; Clynen, E.; Sila, D. N.; Van Loey, A. M.; Hendrickx, M. E. Carrot pectin methylesterase and its inhibitor from kiwi fruit: study of activity, stability and inhibition. *Innovative Food Sci. Emerg. Technol.* **2009**, *10* (4), 601–609.
(29) Bruins, M. E.; Matser, A. M.; Janssen, A. E. A.; Boom, R. M. Buffer selection for HP treatment of biomaterials and its consequences for enzyme inactivation studies. *High Pressure Res.* **2007**, *27* (1), 101–107.
(30) Mahler, H. C.; Friess, W.; Grauschopf, U.; Kiese, S. Protein aggregation: pathways, induction factors and analysis. *J. Pharm. Sci.* **2009**, *98* (9), 2909–2934.
(31) Dirix, C.; Duvetter, T.; Van Loey, A.; Hendrickx, M.; Heremans, K. The in situ observation of the temperature and pressure stability of recombinant *Aspergillus aculeatus* pectin methylesterase with Fourier transform IR spectroscopy reveals an unusual pressure stability of β-helices. *Biochem. J.* **2005**, *392*, 565–571.
(32) Plaza, L.; Duvetter, T.; Van der Plancken, I.; Meersman, F.; Van Loey, A.; Hendrickx, M. Influence of environmental conditions on thermal stability of recombinant *Aspergillus aculeatus* pectinmethylesterase. *Food Chem.* **2008**, *111* (4), 912–920.
(33) Vardhanabhuti, B.; Foegeding, E. A. Effects of dextran sulfate, NaCl, and initial protein concentration on thermal stability of β-lactoglobulin and α-lactalbumin at neutral pH. *Food Hydrocolloids* **2008**, *22* (5), 752–762.
(34) Meersman, F.; Smeller, L.; Heremans, K. Protein stability and dynamics in the pressure−temperature plane. *BBA−Proteins Proteom.* **2006**, *1764* (3), 346–354.
(35) De Cremer, G.; Roeffaers, M. B. J.; Baruah, M.; Sliwa, M.; Sels, B. F.; Hofkens, J.; De Vos, D. E. Dynamic disorder and stepwise deactivation in a chymotrypsin catalyzed hydrolysis reaction. *J. Am. Chem. Soc.* **2007**, *129*, 15458–15459.
(36) Neuman, R. C., Jr.; Kauzmann, W.; Zipp, A. Pressure dependence of weak acid ionization in aqueous buffers. *J. Phys. Chem.* **1973**, *77*, 2687–2691.

Received for review August 18, 2009. Revised manuscript received October 22, 2009. Accepted October 22, 2009. R.P.J. is a Ph.D. Fellow and S.V.B. a Postdoctoral Fellow of the Research Foundation Flanders (FWO). In addition, this study has been carried out with financial support from the Research Fund, K.U.Leuven.